

Empirical Valence-Bond Models for Reactive Potential Energy Surfaces Using Distributed Gaussians

H. Bernhard Schlegel* and Jason L. Sonnenberg

Department of Chemistry, Wayne State University, Detroit, Michigan 48202

Received March 3, 2006

Abstract: A new method for constructing empirical valence bond potential energy surfaces for reactions is presented. Building on the generalized Gaussian approach of Chang–Miller, $V_{12}^2(\mathbf{q})$ is represented by a Gaussian times a polynomial at the transition state and generalized to handle any number of data points on the potential energy surface. The method is applied to two model surfaces and the HCN isomerization reaction. The applications demonstrate that the present method overcomes the divergence problems encountered in some other approaches. The use of Cartesian versus internal or redundant internal coordinates is discussed.

Introduction

In the empirical valence bond (EVB) approach, the potential energy surface (PES) for a reaction in solution is modeled as an interaction between a reactant and a product PES.¹ The interaction between surfaces results in an avoided crossing and yields a smooth function describing the reaction on the ground-state potential energy surface. Good empirical approximations for the noninteracting potential energy surfaces of reactants and products are available from molecular mechanics methods. To obtain a reliable model of a PES for a reaction, a suitable form of the interaction matrix element or resonance integral, $V_{12}(\mathbf{q})$, is needed.

For a two-state system, the interaction between reactant and product surfaces is taken as a modified Morse function in Warshel and Weiss' original multistate EVB method.² The function is adjusted to reproduce barrier heights gleaned from experiments or high-level ab initio calculations, but the form of the surface is not flexible enough to fit frequencies at the transition state (TS). Chang and Miller represented the square of the resonance integral, V_{12}^2 , with a generalized Gaussian.³ The exponents of the Gaussian are chosen to fit the structure and vibrational frequencies of the TS from electronic structure calculations. This form of the EVB surface is sufficiently accurate for molecular dynamics.^{4–12} The Chang–Miller model has also been applied by Jensen^{13,14} and Anglada et al.¹⁵ to transition-state optimizations.

More elaborate functions of the interaction matrix elements were used in the molecular mechanics/valence bond model developed by Bernardi et al. for exploring photochemical reaction potential energy surfaces.¹⁶ Minichino and Voth

generalized the Chang–Miller method³ for N-state systems and provided a scheme to correct gas-phase ab initio data for solutions.¹⁷ Truhlar and co-workers employed a generalized EVB approach by using distance-weighted interpolants to model the interaction matrix elements in their multiconfiguration molecular mechanics method.^{18–20}

The simplicity of the Chang–Miller resonance integral formulation is appealing, but certain difficulties must be overcome to provide the greater flexibility required to model more complex chemical reactions using molecular dynamics. The present article explores two possibilities for improving the representation of the interaction matrix elements. In particular, the generalized Gaussian utilized in the Chang–Miller approach is replaced with a quadratic polynomial times a spherical Gaussian. This avoids the well-known problem caused by negative exponents that may arise in practice.^{12,15,18} Second, to improve the accuracy of the fit, a linear combination of Gaussians times quadratic polynomials placed at suitable locations on the potential energy surface is employed.

Model Description

The EVB model describes a reactive PES in terms of a linear combination of reactant and product wave functions. The coefficients are obtained by solving a simple 2×2 Hamiltonian for the lowest energy.

$$\Psi = c_1\psi_1 + c_2\psi_2 \quad (1)$$

$$\mathbf{H} = \begin{bmatrix} V_{11} & V_{12} \\ V_{21} & V_{22} \end{bmatrix} \quad (2)$$

* Corresponding author. E-mail: hbs@chem.wayne.edu.

$$V_{11} = \langle \psi_1 | \hat{H} | \psi_1 \rangle, \quad V_{12} = V_{21} = \langle \psi_1 | \hat{H} | \psi_2 \rangle, \\ V_{22} = \langle \psi_2 | \hat{H} | \psi_2 \rangle \quad (3)$$

$$V = \frac{1}{2}(V_{11} + V_{22}) - \sqrt{[\frac{1}{2}(V_{11} - V_{22})]^2 + V_{12}^2} \quad (4)$$

Each matrix element is a function of molecular geometry, \mathbf{q} . Good approximations for V_{11} and V_{22} are available from molecular mechanics. However, much less is known about the functional form of the interaction matrix element, V_{12} .

In Warshel and Weiss's approach,² the interaction matrix element V_{12} is chosen to reproduce the barrier height (obtained from experiments or calculations). For cases where greater accuracy is required, it is also desirable to match the position and vibrational frequencies of the TS in addition to the barrier height. The Chang–Miller approach³ describes the interaction matrix element by a generalized Gaussian positioned at or near the transition state

$$V_{12}^2(\mathbf{q}) = A \exp[\mathbf{B}^T \cdot \Delta \mathbf{q} - \frac{1}{2} \Delta \mathbf{q}^T \cdot \mathbf{C} \cdot \Delta \mathbf{q}], \quad \Delta \mathbf{q} = \mathbf{q} - \mathbf{q}_{\text{TS}} \quad (5)$$

where \mathbf{q}_{TS} is the transition-state geometry. The coefficients are chosen so that the energy, gradient, and second derivatives of the EVB surface match ab initio calculations at the TS. Following Chang–Miller's notation,³ this yields simple, closed-form equations for parameters A , \mathbf{B} (a vector), and \mathbf{C} (a matrix).

$$A = [V_{11}(\mathbf{q}_{\text{TS}}) - V(\mathbf{q}_{\text{TS}})][V_{22}(\mathbf{q}_{\text{TS}}) - V(\mathbf{q}_{\text{TS}})] \quad (6a)$$

$$\mathbf{B} = \frac{\mathbf{D}_1}{[V_{11}(\mathbf{q}_{\text{TS}}) - V(\mathbf{q}_{\text{TS}})]} + \frac{\mathbf{D}_2}{[V_{22}(\mathbf{q}_{\text{TS}}) - V(\mathbf{q}_{\text{TS}})]} \text{ and} \\ \mathbf{D}_n = \frac{\partial V_m(\mathbf{q})}{\partial \mathbf{q}} \Big|_{\mathbf{q}=\mathbf{q}_{\text{TS}}} - \frac{\partial V(\mathbf{q})}{\partial \mathbf{q}} \Big|_{\mathbf{q}=\mathbf{q}_{\text{TS}}} \quad (6b)$$

$$\mathbf{C} = \frac{\mathbf{D}_1 \mathbf{D}_1^T}{[V_{11}(\mathbf{q}_{\text{TS}}) - V(\mathbf{q}_{\text{TS}})]^2} + \frac{\mathbf{D}_2 \mathbf{D}_2^T}{[V_{22}(\mathbf{q}_{\text{TS}}) - V(\mathbf{q}_{\text{TS}})]^2} - \\ \frac{\mathbf{K}_1}{V_{11}(\mathbf{q}_{\text{TS}}) - V(\mathbf{q}_{\text{TS}})} - \frac{\mathbf{K}_2}{V_{22}(\mathbf{q}_{\text{TS}}) - V(\mathbf{q}_{\text{TS}})} \text{ and} \\ \mathbf{K}_n = \frac{\partial^2 V_m(\mathbf{q})}{\partial \mathbf{q}^2} \Big|_{\mathbf{q}=\mathbf{q}_{\text{TS}}} - \frac{\partial^2 V(\mathbf{q})}{\partial \mathbf{q}^2} \Big|_{\mathbf{q}=\mathbf{q}_{\text{TS}}} \quad (6c)$$

The original version of the Chang–Miller method runs into difficulties when \mathbf{C} has one or more negative eigenvalues.^{12,15,18} In these cases, the form of V_{12}^2 in eq 5 diverges for large $\Delta \mathbf{q}$ values. The simplest solution to this problem switches the interaction matrix element to zero in regions where the unmodified V_{12}^2 is negative or divergent.¹⁵ Another approach is to include suitable cubic and quartic terms in the Gaussian to control asymptotic behavior.¹²

In the present article, an alternative form for V_{12}^2 is proposed. Instead of using a generalized Gaussian as in eq 5, a quadratic polynomial times a spherical Gaussian is employed.

$$V_{12}^2(\mathbf{q}) = A[1 + \mathbf{B}^T \cdot \Delta \mathbf{q} + \frac{1}{2} \Delta \mathbf{q}^T \cdot (\mathbf{C} + \alpha \mathbf{I}) \cdot \Delta \mathbf{q}] \\ \exp[-\frac{1}{2} \alpha |\Delta \mathbf{q}|^2] \quad (7)$$

Fitting to the energy, gradient, and Hessian at the transition state yields the same formulas for A and \mathbf{B} as those in the

Chang–Miller case; the expression for \mathbf{C} is slightly different.

$$\mathbf{C} = \frac{\mathbf{D}_1 \mathbf{D}_1^T + \mathbf{D}_2 \mathbf{D}_2^T}{A} + \frac{\mathbf{K}_1}{V_{11}(\mathbf{q}_{\text{TS}}) - V(\mathbf{q}_{\text{TS}})} + \\ \frac{\mathbf{K}_2}{V_{22}(\mathbf{q}_{\text{TS}}) - V(\mathbf{q}_{\text{TS}})} \quad (8)$$

The exponent α is chosen to be small enough so that the PES is smooth but not so small that the reactant and product energies are affected significantly. One approach is to choose α to give a good fit for the energies along the reaction path. The form of V_{12}^2 in eq 7 can also be viewed as expanding V_{12}^2 as a linear combination of s-, p-, and d-type Gaussians.

$$g(\mathbf{q}, \mathbf{q}_K, 0, 0, \alpha) = \exp[-\frac{1}{2} \alpha |\mathbf{q} - \mathbf{q}_K|^2]$$

$$g(\mathbf{q}, \mathbf{q}_K, i, 0, \alpha) = (\mathbf{q} - \mathbf{q}_K)_i \exp[-\frac{1}{2} \alpha |\mathbf{q} - \mathbf{q}_K|^2]$$

$$g(\mathbf{q}, \mathbf{q}_K, i, j, \alpha) = (\mathbf{q} - \mathbf{q}_K)_i (\mathbf{q} - \mathbf{q}_K)_j \exp[-\frac{1}{2} \alpha |\mathbf{q} - \mathbf{q}_K|^2] \quad (9)$$

Because the coefficients in eq 7 are linear, the procedure can be readily generalized to include Gaussians at multiple centers, \mathbf{q}_K . For example, one could choose to place the Gaussian centers at the TS, reactant minimum, product minimum, and a few points along the reaction path to either side of the transition state. The generalized form of V_{12}^2 can be written as

$$V_{12}^2(\mathbf{q}) = \sum_K \sum_{i \geq j \geq 0}^{\text{NDim}} B_{ijk} g(\mathbf{q}, \mathbf{q}_K, i, j, \alpha) \quad (10)$$

where NDIM is 3 times the number of atoms for a Cartesian coordinate system or the number of coordinates if internal or redundant-internal coordinates are utilized. The Gaussian exponents are chosen such that the fit is sufficiently smooth for energies along the reaction path and V_{12}^2 is acceptably small at the reactants and products, if these are not already included in \mathbf{q}_K . In the simplest approach, the exponents are all equal; alternatively, if suitable criteria exist, they may be different for different centers, or even for different directions. The B_{ijk} coefficients are obtained by fitting to V_{12}^2 and its first and second derivatives at a number of points, \mathbf{q}_L , which can conveniently be the same as \mathbf{q}_K .

$$V_{12}^2(\mathbf{q}_L) = \sum_K \sum_{i \geq j \geq 0}^{\text{NDim}} B_{ijk} g(\mathbf{q}_L, \mathbf{q}_K, i, j, \alpha) \\ \frac{\partial V_{12}^2(\mathbf{q})}{\partial \mathbf{q}} \Big|_{\mathbf{q}=\mathbf{q}_L} = \sum_K \sum_{i \geq j \geq 0}^{\text{NDim}} B_{ijk} \frac{\partial g(\mathbf{q}, \mathbf{q}_K, i, j, \alpha)}{\partial \mathbf{q}} \Big|_{\mathbf{q}=\mathbf{q}_L} \\ \frac{\partial^2 V_{12}^2(\mathbf{q})}{\partial \mathbf{q}^2} \Big|_{\mathbf{q}=\mathbf{q}_L} = \sum_K \sum_{i \geq j \geq 0}^{\text{NDim}} B_{ijk} \frac{\partial^2 g(\mathbf{q}, \mathbf{q}_K, i, j, \alpha)}{\partial \mathbf{q}^2} \Big|_{\mathbf{q}=\mathbf{q}_L} \quad (11)$$

If the number of Gaussian centers is equal to the number of points (i.e., if the number of coefficients is equal to the number of energy values, first derivatives, and second derivatives), this is simply the solution of a set of linear equations.

$$\mathbf{DB} = \mathbf{F} \quad (12)$$

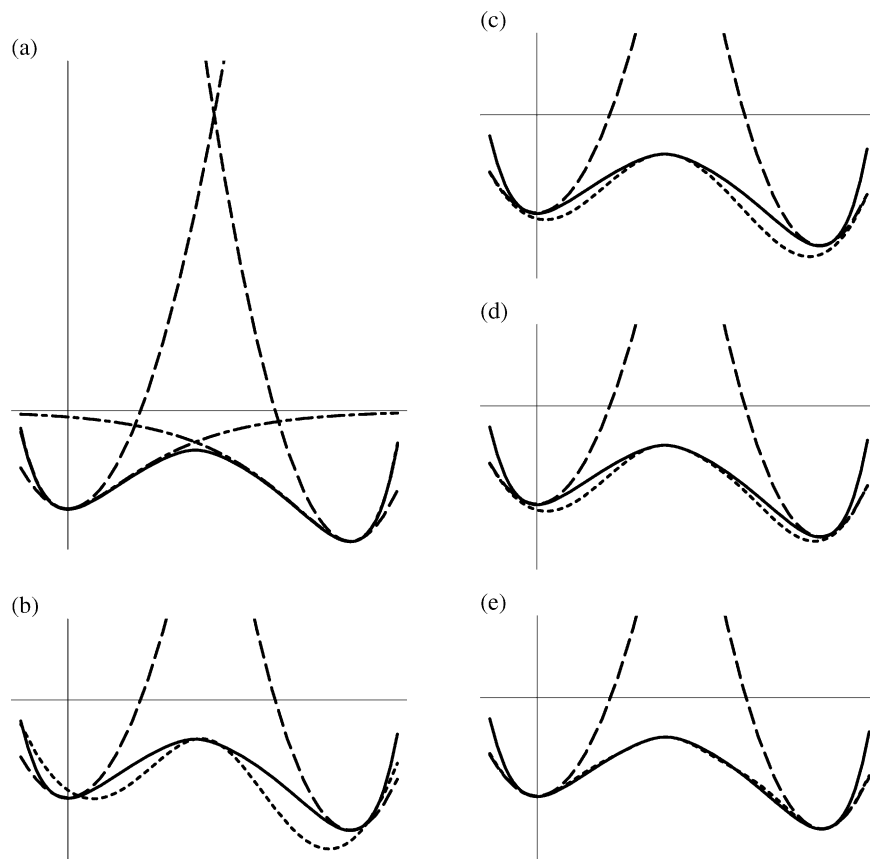


Figure 1. (a) One-dimensional potential energy curve (solid line) constructed from two interacting Morse curves (chain-dot). V_{11} and V_{22} (long dash) are quadratic functions fitted to the minima of the Morse curves, fitted using various EVB models (short dash). (b) EVB model with constant V_{12}^2 . (c) Chang–Miller EVB model with V_{12}^2 represented by a generalized Gaussian. (d) EVB model with V_{12}^2 represented by a quadratic polynomial times a Gaussian. (e) EVB model with a three-Gaussian fit.

where \mathbf{D} is a matrix containing the values of $g(\mathbf{q}_L, \mathbf{q}_K, i, j, \alpha)$, $\partial g(\mathbf{q}_L, \mathbf{q}_K, i, j, \alpha) / \partial \mathbf{q}|_{\mathbf{q}=\mathbf{q}_L}$, and $\partial^2 g(\mathbf{q}_L, \mathbf{q}_K, i, j, \alpha) / \partial \mathbf{q}^2|_{\mathbf{q}=\mathbf{q}_L}$ and \mathbf{F} is a column vector containing the values of $V_{12}^2(\mathbf{q}_L)$, $\partial V_{12}^2(\mathbf{q}) / \partial \mathbf{q}|_{\mathbf{q}=\mathbf{q}_L}$, and $\partial^2 V_{12}^2(\mathbf{q}) / \partial \mathbf{q}^2|_{\mathbf{q}=\mathbf{q}_L}$. Even with only a few expansion centers, the eigenvalues of \mathbf{D} become very small because of strong overlap between the Gaussians. In this case, the coefficients can be chosen in a least-squares manner. Similarly, if the number of Gaussian centers in the expansion is chosen to be smaller than the number of points where V_{12}^2 and its derivatives are evaluated, then the coefficients can also be obtained in a least-squares manner.

$$\begin{aligned} \text{minimize}(\mathbf{DB} - \mathbf{F})^T \mathbf{W} (\mathbf{DB} - \mathbf{F}) \\ \mathbf{D}^T \mathbf{W} \mathbf{D} \mathbf{B} = \mathbf{D}^T \mathbf{W} \mathbf{F} \end{aligned} \quad (13)$$

where \mathbf{W} is a diagonal weighting matrix. This can be solved easily using singular value decomposition.

Examples

One-Dimensional Test Case—Intersecting Morse Curves. A simple one-dimensional potential energy curve can be constructed from two intersecting Morse curves, as shown in Figure 1a. This resembles the potential energy along the reaction path for hydrogen abstraction reactions, $X-H + Y \rightarrow X + H-Y$, and similar atom-transfer processes involving the forming and breaking of single bonds. The parameters for the Morse curves are $D_e = 0.12$ and 0.16 au with force constants at the minima of 0.40 and 0.50 au, respectively; the curves are displaced by 3.00 au and interact by a small

matrix element, $V_{12}^2 = 0.010$ au. The empirical valence bond approximation to the surface is constructed from two quadratic potentials fitted to the individual Morse functions at their minima. As can be seen from Figure 1a, in the region of the transition state, V_{11} and V_{22} are much higher than the potential energy curve being modeled. Hence, V_{12}^2 will have to be quite large, providing a suitable challenge for the methodology.

Starting with Warshel and Weiss's method,² V_{12}^2 is set equal to a constant. In Figure 1b, the constant is chosen to reproduce the forward barrier height, and the curve is displaced to match the energies of the reactant and TS. Note that the resulting minima positions are shifted, the barrier width is too small, and the reaction exothermicity is too large. With only one parameter, fitting the potential energy curve well is difficult.

In the Chang–Miller approach, V_{12}^2 is represented by a generalized Gaussian, with the parameters fitted to the transition-state energy, gradient, and Hessian. For this example, the parameters for eq 5 are $A = 0.167$, $\mathbf{B} = 0.385$, and $\mathbf{C} = 1.988$. As shown in Figure 1c, this yields a significant improvement in fit to the potential energy curve. Because V_{12}^2 is not zero at the reactant and product geometries, the minima are slightly displaced, though not as much as in Figure 1b. When V_{12}^2 is represented by a single Gaussian times a quadratic polynomial, Figure 1d, the results are similar to the Chang–Miller approach. The Gaussian exponent α can be varied over the range 1.5 – 3.0 (bracketing the Chang–Miller

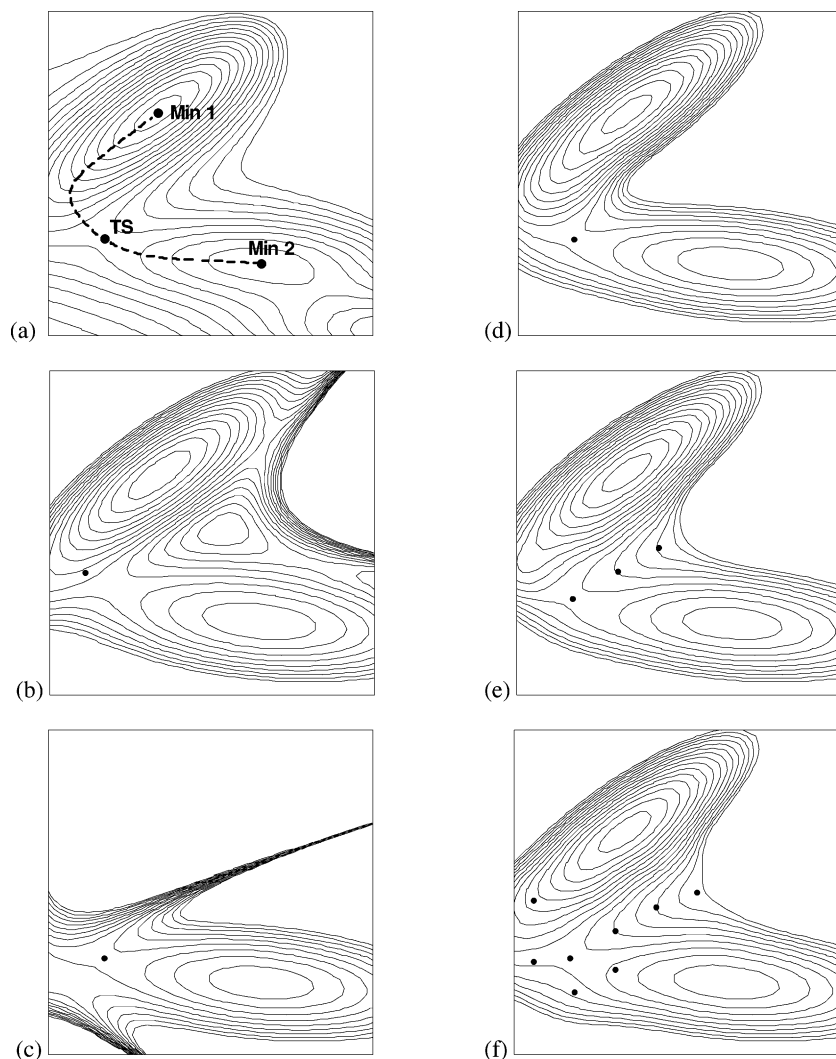


Figure 2. (a) Müller–Brown potential. (b) Chang–Miller EVB model with the V_{12}^2 Gaussian placed at the minimum on the intersection seam of V_{11} and V_{22} . (c) Chang–Miller EVB model with the V_{12}^2 Gaussian at the TS. (d) EVB model with V_{12}^2 represented by a quadratic polynomial times a Gaussian at the TS. (e) EVB model with a three-Gaussian fit. (f) EVB model with an eight-Gaussian fit. In parts b–f, the points indicate positions of the Gaussians used to construct V_{12}^2 .

exponent) and provides some additional flexibility in fitting the potential. If the exponent is chosen to be too large, V_{12}^2 is too narrow and the EVB curve no longer descends smoothly from the transition state.

A better fit is obtained by using three Gaussians times quadratic polynomials, for example, one at the transition state, another halfway between the TS and the reactant, and the third halfway between the TS and the product. Figure 1e shows that this approach produces a very good fit to the potential energy curve for suitably chosen exponents. The additional two Gaussians could also be placed at the minima, but this does not yield as smooth a curve. For more difficult cases, it could be beneficial to utilize five Gaussians: one at the TS, one at each minimum, and one halfway between the TS and each minimum.

Two-Dimensional Test Case—Müller–Brown Surface. The Müller–Brown surface²¹ is a convenient two-dimensional example frequently used as a test case for optimization algorithms and reaction-path-following methods:

$$V(x,y) = \sum A_i \exp[a_i(x - x_i^0)^2 + b_i(x - x_i^0)(y - y_i^0) + c_i(y - y_i^0)^2] \quad (14)$$

where $A = \{-200, -100, -170, 15\}$, $x^0 = \{1, 0, -0.5, -1\}$, $y^0 = \{0, 0.5, 1.5, 1\}$, $a = \{-1, -1, -6.5, 0.7\}$, $b = \{0, 0, 11, 0.6\}$, and $c = \{-10, -10, -6.5, 0.7\}$. As shown in Figure 2a, the surface has three minima. The upper two minima are connected by a rather curved reaction path and serve as a suitable test case for the EVB model. The V_{11} and V_{22} potentials are chosen as quadratic functions fitted to these two minima. Figure 2b demonstrates that the Chang–Miller method produces a good representation of the surface when the Gaussian for V_{12}^2 is placed at the lowest point on the intersection seam of V_{11} and V_{22} . Bofill et al. has used this approach in modeling potential energy surfaces for transition-state optimizations.¹⁵ However, placing a Gaussian for the Chang–Miller method at the TS yields a very poor approximation of the Müller–Brown surface, as seen in Figure 2c. This is because the matrix C has one negative eigenvalue, causing V_{12}^2 to diverge along the corresponding direction.

If V_{12}^2 is represented by a Gaussian times a quadratic polynomial placed at the transition state, then a good approximation to the Müller–Brown surface is obtained, as shown in Figure 2d. A better fit to the ridge separating the two minima may be constructed by placing two additional

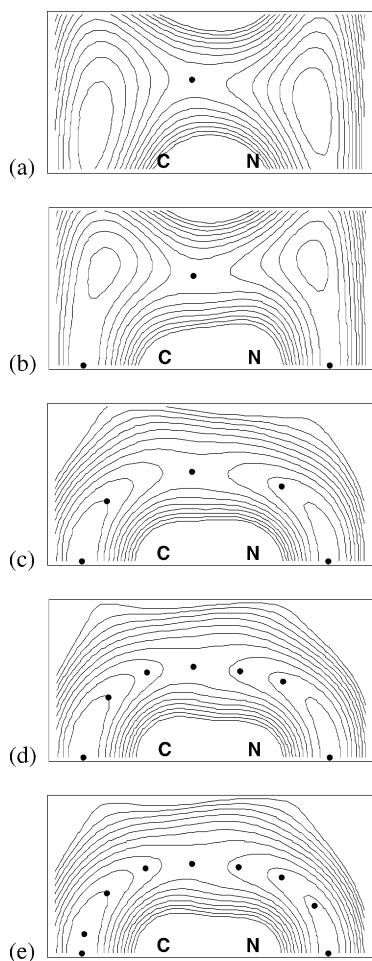


Figure 3. EVB fit to the potential energy surface for $\text{HCN} \rightarrow \text{HNC}$ using a Gaussian times a polynomial for V_{12}^2 in Cartesian coordinates. The carbon is at the origin; the nitrogen is at (1.116, 0.000), and the energy is plotted as a function of the Cartesian coordinates of the hydrogen. The points in a–e indicate the positions of the Gaussians used to construct V_{12}^2 .

Gaussians along the ridge, Figure 2e. The surface can be improved further by including more Gaussians, Figure 2f.

Molecular Case— $\text{HCN} \rightarrow \text{HNC}$. The isomerization of hydrogen cyanide is a simple unimolecular reaction often employed to test potential energy surface exploring algorithms. Because the C–N bond length changes little during this process, the key components of the potential energy surface can be easily visualized in two dimensions by plotting energy as a function of the hydrogen position. In internal coordinates involving bond lengths and angles, the reaction path is relatively linear. However, if Cartesian coordinates are used for the hydrogen, the reaction path is approximately a semicircle and fitting the surface should be more challenging. In particular, an EVB model with V_{11} , V_{22} , and V_{12}^2 in Cartesian coordinates is better suited for straight valleys rather than curved paths.

The transition state and reaction path for the $\text{HCN} \rightarrow \text{HNC}$ surface were calculated using the HF/3-21G level of theory.^{22–26} First and second derivatives were calculated at the transition state, the two minima, and selected points along the reaction path as input for the EVB model. The results are shown in Figure 3. Applying a Gaussian times a polynomial at the transition state yields a surface with some problems, Figure 3a. As a result of using Cartesian coordi-

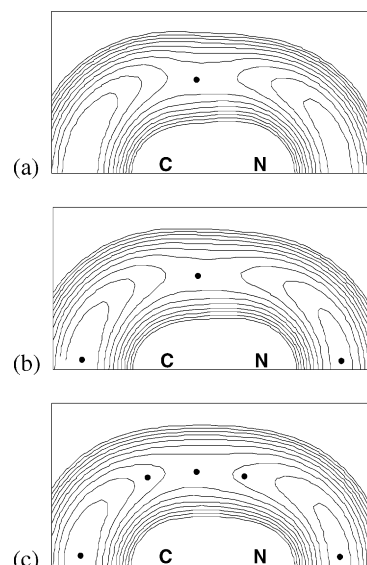


Figure 4. EVB fit to the potential energy surface for $\text{HCN} \rightarrow \text{HNC}$ using harmonic functions for V_{11} and V_{22} in redundant internal coordinates (C–N stretch, C–H stretch, N–H stretch, $\angle\text{H–C–N}$ bend, and $\angle\text{H–N–C}$ bend) using a Gaussian times a polynomial for V_{12}^2 in redundant internal coordinates. The carbon is at the origin; the nitrogen is at (1.116, 0.000), and the energy is plotted as a function of the Cartesian coordinates of the hydrogen. The points in a–c indicate the positions of Gaussians used to construct V_{12}^2 .

nates for the EVB surface, the minima valleys do not curve toward the transition state. The minima appear to have moved off the C–N axis as a consequence of fitting the V_{12}^2 only at the transition state. When two additional Gaussians ($\alpha = 0.5$) at the minima are included, Figure 3b, the energy, gradients, and Hessians at the minima are reproduced correctly by the EVB surface. However, the valleys still do not properly curve toward the TS, and there are spurious minima for bent structures. Adding two more points between the TS and the minima, Figure 3c, corrects the curvature of the valleys and eradicates the spurious minima. Two additional points near the transition state serve to improve the width of the potential energy surface through the transition state, Figure 3d. Extra points near the minima, Figure 3e, do not seem to provide any additional improvement.

As an alternative to Cartesian coordinates, internal coordinates can be used to construct V_{11} and V_{22} and to fit V_{12}^2 . Internal coordinates are more natural coordinates for this surface with a curved reaction path than Cartesian coordinates. To include the coordinates appropriate for both reactants and products, a redundant internal coordinate system consisting of $R(\text{CN})$, $R(\text{CH})$, $R(\text{NH})$, $\angle\text{HCN}$, and $\angle\text{HNC}$ was chosen. The simple Chang–Miller approach had difficulties because of negative eigenvalues in \mathbf{C} . A Gaussian times a quadratic polynomial provided a very reasonable fit to the surface, as shown in Figure 4a. Adding Gaussians near the reactant and product minima improves the surface somewhat, Figure 4b, primarily by providing a better fit around the minima. With an α value of 0.8 au for all Gaussians, the maximum error in the energy for points along the reaction path is 0.0025 au. Including two additional points along the reaction path on either side of the transition state reduced this error by a factor of 10 (Figure 4c, $\alpha = 1.5$ au).

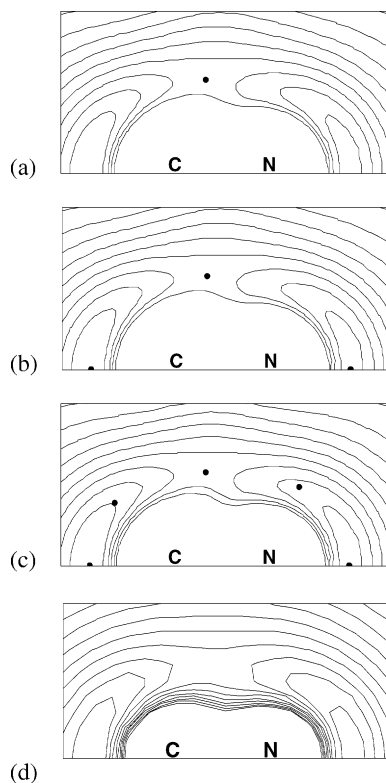


Figure 5. EVB fit using anharmonic functions for V_{11} and V_{22} in nonredundant (Z-matrix) internal coordinates (Morse for stretch, harmonic for bend, LJ for repulsion) and Gaussians times a polynomial in Cartesian coordinates for V_{12}^2 . The carbon is at the origin; the nitrogen is at (1.116, 0.000), and the energy is plotted as a function of the Cartesian coordinates of the hydrogen. The points in a–c indicate the positions of the Gaussians used to construct V_{12}^2 . (d) The potential energy surface for $\text{HCN} \rightarrow \text{HNC}$ calculated at RHF/3-21G.

Further reduction in the error can be achieved by adding more Gaussian centers at appropriate places on the surface.

As can be seen from Figures 3 and 4, the choice for V_{11} and V_{22} clearly has a profound effect on the shape of the potential energy surface in the regions away from the reaction path and fitting points. The simple harmonic functions used in Figures 3 and 4 were chosen to challenge the fitting procedure. More realistic potentials employed in molecular mechanics force fields include anharmonic stretching and bending potentials and nonbonded repulsions. Results employing such potentials are summarized in Figure 5 and compared to the actual $\text{HCN} \rightarrow \text{HNC}$ surface obtained by calculating the energy at the HF/3-21G level of theory on a suitable grid of points depicted in Figure 5d. To represent V_{11} in HCN, we employed Morse functions for the CN and CH bond stretches, harmonic potentials for the HCN bend and the CN–CH stretch–stretch interaction, and Lennard-Jones potentials for the nonbonded N–H interaction (an anti-Morse function works just as well; alternatively, a suitable anharmonic bend could have been used). Although the N–H nonbonded interaction would normally be covered by anharmonic bending terms in conventional force fields, a Lennard-Jones potential was employed to test the robustness of our fitting procedure. The corresponding coordinates were used in V_{22} for HNC. The interaction matrix element, V_{12}^2 , was represented by one or more Gaussians times polynomials in Cartesian coordinates and fit to energies, Cartesian

gradients, and Cartesian Hessians at selected points along the reaction path. A very good EVB surface is obtained with V_{12}^2 fit by only a single Gaussian times a quadratic polynomial at the transition state. The minima and shape of the reaction path are represented well. With suitably chosen dissociation energies for the Morse, the asymptotic form of the surface is also reproduced well. Including Gaussians at the minima does not change the surface, but adding two additional points between the minima and the TS improves the EVB surface. For the EVB surfaces shown Figure 5c, V_{12}^2 fit by five Gaussians with an exponent of 0.7 au yields a maximum error of 0.00013 au for the energy for points along the reaction path.

The logical extension of the tests cases illustrated in Figures 3–5 is the combination of anharmonic potentials for V_{11} and V_{22} in the natural internal coordinates for the reactants and products and V_{12}^2 represented by a series of Gaussians times quadratic polynomials in redundant internal coordinates. As in the quadratic synchronous transit transition-state optimization procedures,²³ these redundant internal coordinates are best chosen as the union of the reactant and product internal coordinates, augmented by any additional internal coordinates required to represent interactions found only in the reactive region of the potential energy surface. For an improved fit to V_{12}^2 , the Gaussians at the reactants, products, and transition states (and possible intermediates along the reaction path) should be augmented by additional Gaussians placed between those stationary points and the transition states along the reaction path. Extra fitting points can be added to represent special features such as the tunneling region near a saddle point or extended ridges separating reactant and product valleys. Molecular dynamics can locate additional areas of the potential energy surface where extra fitting points may be needed, in a manner akin to the “GROW” procedure of Collins.²⁷

Summary

The present work investigates some alternatives for representing V_{12}^2 employed in constructing EVB-type potential energy surfaces for later use in molecular dynamics calculations of chemical reactions. The use of a Gaussian times a quadratic polynomial for V_{12}^2 instead of the generalized Gaussian used in the Chang–Miller method has been proposed. This approach overcomes the divergence difficulties often encountered in practice when the generalized Gaussian is used to fit to the energy, gradient, and Hessian at a transition state. The approach is extended by representing V_{12}^2 as a linear combination of Gaussians times polynomials at selected points anywhere on the surface. The utility of the methodology is illustrated by applications to some simple one- and two-dimensional model surfaces along with the surface for the $\text{HCN} \rightarrow \text{HNC}$ isomerization reaction. A single Gaussian times a quadratic polynomial performs as well as the Chang–Miller approach where the latter succeeds and gives a good fit even when Chang–Miller has divergence difficulties. Better fits to potential energy surfaces are obtained with a distribution of Gaussians, particularly when the reaction path is curved or when the coordinates system makes the fit challenging. For $\text{HCN} \rightarrow \text{HNC}$, the effect of

the coordinate system on the quality of the EVB surface was explored. Internal coordinates performed better than Cartesian coordinates; however, both coordinate systems could be used to fit the potential energy along the reaction path to within chemical accuracy with as few as five fitting points. The quality of the surface away from the fitting points depends on the choice of V_{11} and V_{22} . Anharmonic, internal coordinate potentials with the proper asymptotic behavior produce a significantly improved global surface when compared to harmonic potentials in either Cartesian or internal coordinates. There is no restriction on the coordinate system or placement of the Gaussians representing V_{12}^2 in the current method, and extra points can be added to fine-tune special features on the surface. Practical methods for the automatic placement of the Gaussians will be explored in future work.

Acknowledgment. This research was supported by the Office of Naval Research (N00014-05-1-0457). The authors thank Drs. W. H. Miller, G. A. Voth, K. Wong, and F. Paesani for helpful discussions.

References

- (1) Villa, J.; Warshel, A. *J. Phys. Chem. B* **2001**, *105*, 7887–7907.
- (2) Warshel, A.; Weiss, R. M. *J. Am. Chem. Soc.* **1980**, *102*, 6218–6226.
- (3) Chang, Y.-T.; Miller, W. H. *J. Phys. Chem.* **1990**, *94*, 5884–5888.
- (4) Hansson, T.; Nordlund, P.; Aqvist, J. *J. Mol. Biol.* **1997**, *265*, 118–127.
- (5) Okuyama-Yoshida, N.; Nagaoka, M.; Yamabe, T. *J. Phys. Chem. A* **1998**, *102*, 285–292.
- (6) Nagaoka, M.; Okuyama-Yoshida, N.; Yamabe, T. *J. Phys. Chem. A* **1998**, *102*, 8202–8208.
- (7) Luzhkov, V.; Aqvist, J. *J. Am. Chem. Soc.* **1998**, *120*, 6131–6137.
- (8) Okuyama-Yoshida, N.; Kataoka, K.; Nagaoka, M.; Yamabe, T. *J. Chem. Phys.* **2000**, *113*, 3519–3524.
- (9) Karmacharya, R.; Antoniou, D.; Schwartz, S. D. *J. Phys. Chem. A* **2001**, *105*, 2563–2567.
- (10) Aqvist, J.; Warshel, A. *Chem. Rev.* **1993**, *93*, 2523–2544.
- (11) Hwang, J. K.; Chu, Z. T.; Yadav, A.; Warshel, A. *J. Phys. Chem.* **1991**, *95*, 8445–8448.
- (12) Chang, Y. T.; Minichino, C.; Miller, W. H. *J. Chem. Phys.* **1992**, *96*, 4341–4355.
- (13) Jensen, F. *J. Comput. Chem.* **1994**, *15*, 1199.
- (14) Jensen, F. *J. Am. Chem. Soc.* **1992**, *114*, 1596.
- (15) Anglada, J. M.; Besalu, E.; Bofill, J. M.; Crehuet, R. *J. Comput. Chem.* **1999**, *20*, 1112–1129.
- (16) Bernardi, F.; Olivucci, M.; Robb, M. A. *J. Am. Chem. Soc.* **1992**, *114*, 1606–1616.
- (17) Minichino, C.; Voth, G. A. *J. Phys. Chem. B* **1997**, *101*, 4544–4552.
- (18) Kim, Y.; Cochado, J. C.; Villa, J.; Xing, J.; Truhlar, D. G. *J. Chem. Phys.* **2000**, *112*, 2718–2735.
- (19) Lin, H.; Pu, J.; Albu, T. V.; Truhlar, D. G. *J. Phys. Chem. A* **2004**, *108*, 4112–4124.
- (20) Albu, T. V.; Cochado, J. C.; Truhlar, D. G. *J. Phys. Chem. A* **2001**, *105*, 8465–8487.
- (21) Müller, K.; Brown, L. D. *Theor. Chim. Acta* **1979**, *53*, 75.
- (22) Frisch, M. J.; Trucks, G. W.; Schlegel, H. B.; Scuseria, G. E.; Robb, M. A.; Cheeseman, J. R.; Montgomery, J. A., Jr.; Vreven, T.; Kudin, K. N.; Burant, J. C.; Millam, J. M.; Iyengar, S. S.; Tomasi, J.; Barone, V.; Mennucci, B.; Cossi, M.; Scalmani, G.; Rega, N.; Petersson, G. A.; Nakatsuji, H.; Hada, M.; Ehara, M.; Toyota, K.; Fukuda, R.; Hasegawa, J.; Ishida, M.; Nakajima, T.; Honda, Y.; Kitao, O.; Nakai, H.; Klene, M.; Li, X.; Knox, J. E.; Hratchian, H. P.; Cross, J. B.; Adamo, C.; Jaramillo, J.; Gomperts, R.; Stratmann, R. E.; Yazyev, O.; Austin, A. J.; Cammi, R.; Pomelli, C.; Ochterski, J. W.; Ayala, P. Y.; Morokuma, K.; Voth, G. A.; Salvador, P.; Dannenberg, J. J.; Zakrzewski, V. G.; Dapprich, S.; Daniels, A. D.; Strain, M. C.; Farkas, O.; Malick, D. K.; Rabuck, A. D.; Raghavachari, K.; Foresman, J. B.; Ortiz, J. V.; Cui, Q.; Baboul, A. G.; Clifford, S.; Cioslowski, J.; Stefanov, B. B.; Liu, G.; Liashenko, A.; Piskorz, P.; Komaromi, I.; Martin, R. L.; Fox, D. J.; Keith, T.; Al-Laham, M. A.; Peng, C. Y.; Nanayakkara, A.; Challacombe, M.; Gill, P. M. W.; Johnson, B.; Chen, W.; Wong, M. W.; Gonzalez, C.; Pople, J. A. *Gaussian 03*, revision B.03 ed.; Gaussian, Inc.: Wallingford, CT, 2004.
- (23) Peng, C.; Schlegel, H. B. *Isr. J. Chem.* **1993**, *33*, 449–454.
- (24) Gonzalez, C.; Schlegel, H. B. *J. Phys. Chem.* **1990**, *94*, 5523.
- (25) Gonzalez, C.; Schlegel, H. B. *J. Chem. Phys.* **1989**, *90*, 2145.
- (26) Binkley, J. S.; Pople, J. A.; Hehre, W. J. *J. Am. Chem. Soc.* **1980**, *102*, 939–947.
- (27) Collins, M. A. *Theor. Chem. Acc.* **2002**, *108*, 313–324.

CT600084P